PERGAMON

Corrosion Science 43 (2001) 157–170

CORROSION SCIENCE

www.elsevier.com/locate/corsci

Inhibition of 5083 aluminium alloy and galvanised steel by lanthanide salts

M.A. Arenas [a], M. Bethencourt [b], F.J. Botana [b], J. de Damborenea [a,*], M. Marcos [c]

[a] *Departamento de Corrosión y Protección, Centro Nacional de Investigaciones Metalúrgicas (CENIM/CSIC), Avenida de Gregorio del Amo 8, E-28040 Madrid, Spain*

[b] *Departamento de Ciencia de los Materiales e Ingeniería Metalúrgica y Química Inorgánica, Facultad de Ciencias del Mar, Universidad de Cádiz, Polígono Río San Pedro s/n, Apto. 40, Puerto Real, 11510 Cádiz, Spain*

[c] *Departamento Ingenieria Mecánica y Diseño Industrial, Universidad de Cádiz, Escuela Superior de Ingeniería, c/Chile s/n, 11003 Cádiz, Spain*

Received 1 March 2000; accepted 10 April 2000

Abstract

Lanthanide salts are being considered as an environmentally friendly alternative to the classic systems based on chromates. The inhibitor behaviour of $CeCl_3$ has been studied for both AA5083 alloy and galvanised steel in aerated NaCl solutions. For AA5083, cerium appears as dispersed islands whilst in the galvanised steel samples, it is stochastically dispersed onto the metallic surface, forming a film. These differences can be interpreted in terms of the distribution of cathodic areas for each material. In the case of AA5083, Al_6–(Mn,Fe,Cr) acts as permanent cathodic site whilst permanent cathodic sites do not exist in the galvanised steel. © 2000 Elsevier Science Ltd. All rights reserved.

Keywords: Cerium salts; Green inhibitor; Galvanised steel; Aluminium alloy; Corrosion

1. Introduction

New environmental restrictions have particularly affected the industry of surface treatment and finishing of metals [1]. To this effect, the need to search for

* Corresponding author. Fax: +34-91-534-7425.
E-mail address: jdambo@fresno.csic.es (J. de Damborenea).

0010-938X/00/$ - see front matter © 2000 Elsevier Science Ltd. All rights reserved.
PII: S0010-938X(00)00051-2

non-contaminating alternatives for the process of anticorrosion treatments based on chromates has arisen [2].

The use of rare earth metals has been proposed in the literature [3–9]. According to previous works, the mechanism of action of the rare earth elements is based on blocking the cathodic areas of the material, reducing the rate of the cathodic process and, as a consequence, that of the associated anodic process.

This paper presents the study of the inhibitor effect of $CeCl_3$ against the corrosion in sea water of galvanised steel and an aluminium–magnesium alloy. The differences observed in the behaviour of the inhibitor will be analysed, fundamentally, based on the mechanisms of corrosion/inhibition that occur in both systems.

2. Experimental

Samples of a commercially galvanised steel of $90 \times 50 \times 1$ mm^3 (hot dip galvanised at 450° for 1 min) and samples of an AA5083 alloy of $30 \times 25 \times 3$ mm^3 were used. The composition of both these materials are given in Table 1.

The microstructrural characterisation of the two types of specimens was carried out by means of optical microscopy (OM), scanning electron microscopy (SEM) and energy dispersive spectroscopy (EDS). A 3.5 wt.% NaCl solution, saturated in oxygen, was used as an electrolyte. To evaluate the inhibitor effect of lanthanide salts, variable concentrations of $CeCl_3 \cdot 7H_2O$ from 100 to 1000 ppm were added to the NaCl solution.

The behaviour of the materials was studied by means of electrochemical tests. The linear potentiodynamic polarisation curves were measured at room temperature with a 1286 Solartron potentiostat controlled by a PC and with a potential sweep rate of 10 mV min^{-1}. A three-electrode cell was used in these tests. The working electrode is the material to be studied, the reference is an Ag–AgCl electrode and graphite is used as a counter electrode.

3. Results and discussion

3.1. Corrosion of AA5083 alloy in 3.5% NaCl solution

The study carried out by means of SEM and EDS of AA5083 shows three intermetallic compounds distributed unevenly on the aluminium matrix. These inter-

Table 1
Composition of studied materials

Composition	Mg	Mn	Si	Fe	Ti	Cu	Cr	Pb	Zn	Al
AA5083	4.9	0.5	0.13	0.30	0.03	0.08	0.13	–		Balance
Zn bath for galvanised steel	–	–	–	–	–	–	–	0.004	Balance	0.01

metallics are mainly composed of Al_6–(Mn,Fe,Cr), Al–Mg and of Al–(Si,Mg), in agreement with the literature [10,11]. Besides the difference in composition, these precipitates also display notable differences in size and abundance. The precipitates with the largest average size (~50 μm^2) and greatest abundance are those of Al–(Mn,Fe,Cr). On the other hand, the smallest are those of Al–Mg (~6 μm^2), while the intermediate precipitates are those of Al–(Si,Mg) (~30 μm^2). The cathodic or anodic character of these precipitates with respect to the aluminium matrix will determine the type of corrosion of the alloy [12].

Fig. 1(a) presents the metallographic structure of the Al alloy, showing the Al_6–(Mn,Fe,Cr) and Al–(Si,Mg) intermetallics. Fig. 1(b) contains the image of the same area of this sample after 72 h of immersion in the 3.5% NaCl solution. When comparing both images, it is possible to observe that a process of local corrosion has occurred in the surrounding area of the Al_6–(Mn,Fe,Cr) precipitates. Meanwhile, the Al–(Si,Mg) particles remain unaffected.

These results can be explained based on the cathodic or anodic character of both intermetallic compounds. Indeed, the Al_6–(Mn,Fe,Cr) precipitates are more cathodic than the aluminium matrix [13]. Hence, these precipitates are converted into permanent cathodes, with the reduction of oxygen to OH^- ions taking place [14]. This causes a local increase of the pH, resulting in the dissolution of the oxide layer surrounding the precipitates. Once this layer has dissolved, the local increase in alkalinity causes an intense attack on the matrix.

On the other hand, the images in Fig. 1 suggest that the intermetallic compounds of Al–(Si,Mg), as well as those of Al–Mg, have an electrochemical activity similar to that of the matrix [15]; this would justify the absence of attack on them or on the surrounding matrix. In accordance with all the above-mentioned discussions, the corrosion of the AA5083 alloy in the NaCl solution would be characterised by the existence of a local increase in alkalinity in the areas corresponding to the precipitates of Al_6–(Mn,Fe,Cr). This process causes the break up of the oxide layer in their surrounding area, and then in the matrix that surrounds the precipitates.

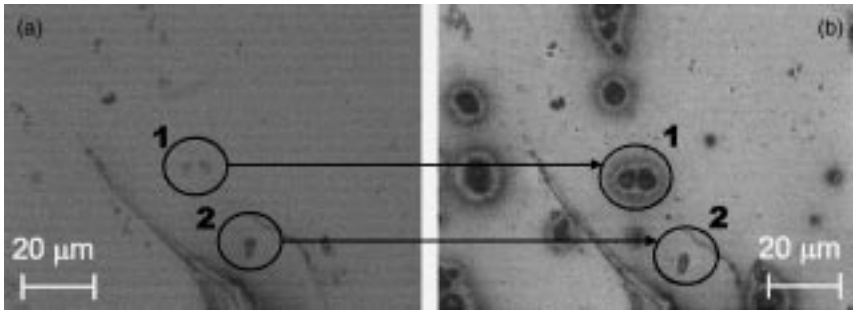

Fig. 1. (a) SEM micrograph of aluminium alloy and (b) the attacked area surrounding the Al_6–(Mn,Fe,Cr) and Al–(Si,Mg) intermetallics, marked as 1 and 2 in the image, after 72 h in NaCl solution can be distinguished.

3.2. Corrosion of the galvanised steel in 3.5% NaCl solution

In general, in the galvanised steel, a simple visual inspection allows one to observe large crystals of zinc forming the characteristic spangle. Fig. 2(a) shows an SEM micrograph of the surface of a galvanised sample in which a distribution of hexagonal grains of approximately the same size can be observed. At the grain boundaries

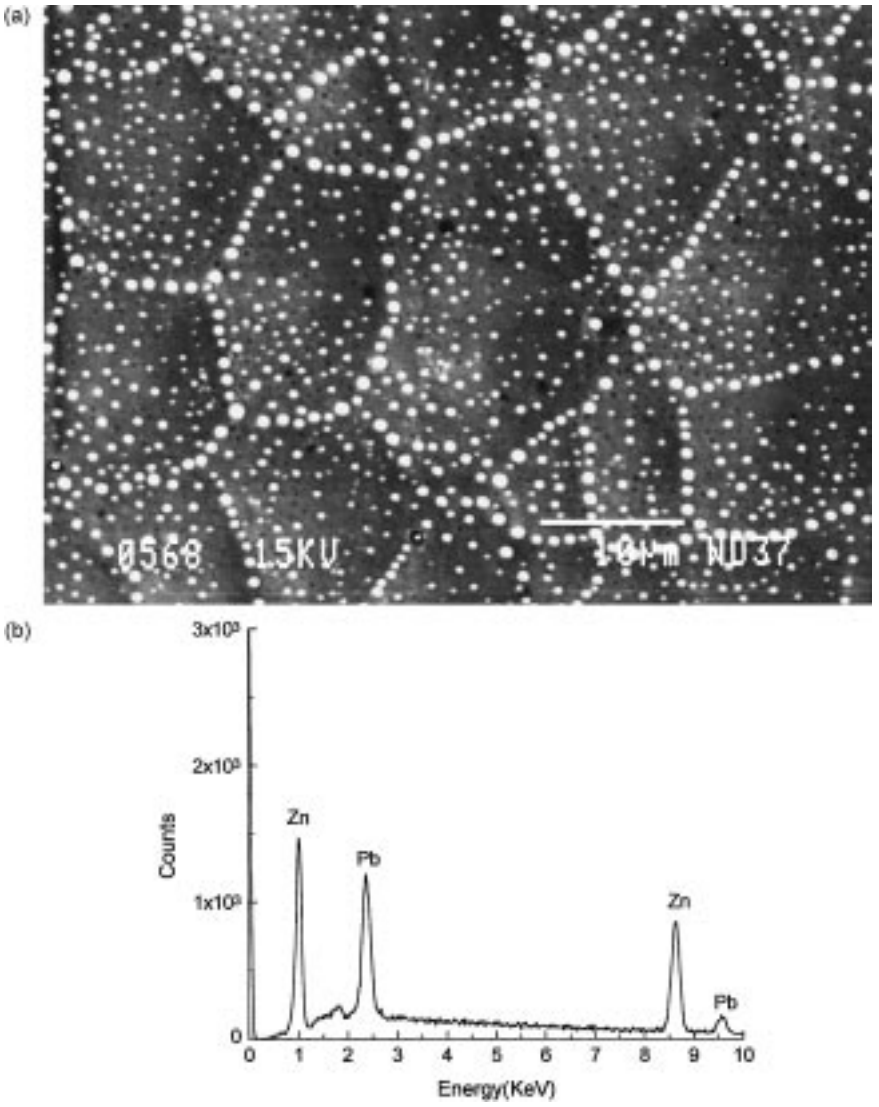

Fig. 2. (a) SEM image of galvanised steel and (b) EDS spectrum of the white points at the grain boundaries and inside the grains showing a high Pb content.

as well as inside the grains, some white points could be seen, whose analysis revealed a high content of lead as is depicted in Fig. 2(b). These precipitates are rich in Pb as a consequence of the segregation of insoluble elements in the surface, as was pointed out by other authors [16]. The lead is added to the galvanisation bath with the aim of increasing the fluency of zinc and producing the characteristic spangle finish. However, the excess of Pb in the bath separates and deposits at the bottom, avoiding the iron slag sticking to the pot, facilitating its cleaning [17–19].

At present, the quantity of this element and others such as Cd or Sn in the bath is controlled since it has been observed that their presence as sludge could cause the phenomenon of intergranular corrosion of the galvanised steel [20]. In principle (similar to what happens to the precipitates of Al–(Mn,Fe) in the AA5083 alloy), owing to the difference in electrochemical activity between the particles with a high lead content and the rest of the surface, they could be thought of as permanent cathodes for the galvanised steel.

The samples immersed in 3.5% NaCl solution for 30 days present a voluminous layer of white corrosion products on the surface. This layer has a spongy texture that, when magnified, reveals a structure formed by an accumulation of needles rich in Zn (Fig. 3). This morphology is characteristic of the corrosion products formed on the external zinc-rich layer. When the layer of corrosion products developed on the surface of the galvanised steel was eliminated, localised corrosion was not observed, contrary to what happened for the AA5083 alloy (Fig. 1). However, the interstitial localisation of the lead can cause tension in the crystalline lattice, creating greater heterogeneity in the surface, and therefore increasing the surface activity. According to these observations, we could discard the idea that the lead precipitates are permanent cathodes, and just a random distribution of cathodic and anodic areas should produce an uniform corrosion process as it is presented in Fig. 4.

Therefore, while under the studied conditions the samples of the AA5083 alloy are corroded by a local process, the galvanised steel undergoes uniform corrosion.

3.3. The use of $CeCl_3$ as an inhibitor

The linear polarisation curves obtained for the galvanised steel and for the AA5083 alloy in the NaCl solution are represented in Fig. 5. In both cases, the predominant cathodic reaction, where oxygen is reduced, is the rate controlling stage of the process of corrosion.

Nevertheless, it is convenient to highlight the differences between the anodic branches of the linear polarisation curves for both systems. While the galvanised steel shows a high activity associated with the dissolution of the zinc, the AA5083 alloy possesses a region of imperfect passivity of the order of 50 mV.

Therefore, since the reaction step that determines the rate of the process of corrosion is the cathodic one in both systems, it would seem advisable to use a cathodic inhibitor as a starting point for the design of the protection systems. This type of inhibitor acts by blocking the cathodic areas of the material, reducing its rate and, in consequence, that of the anodic process [22–25].

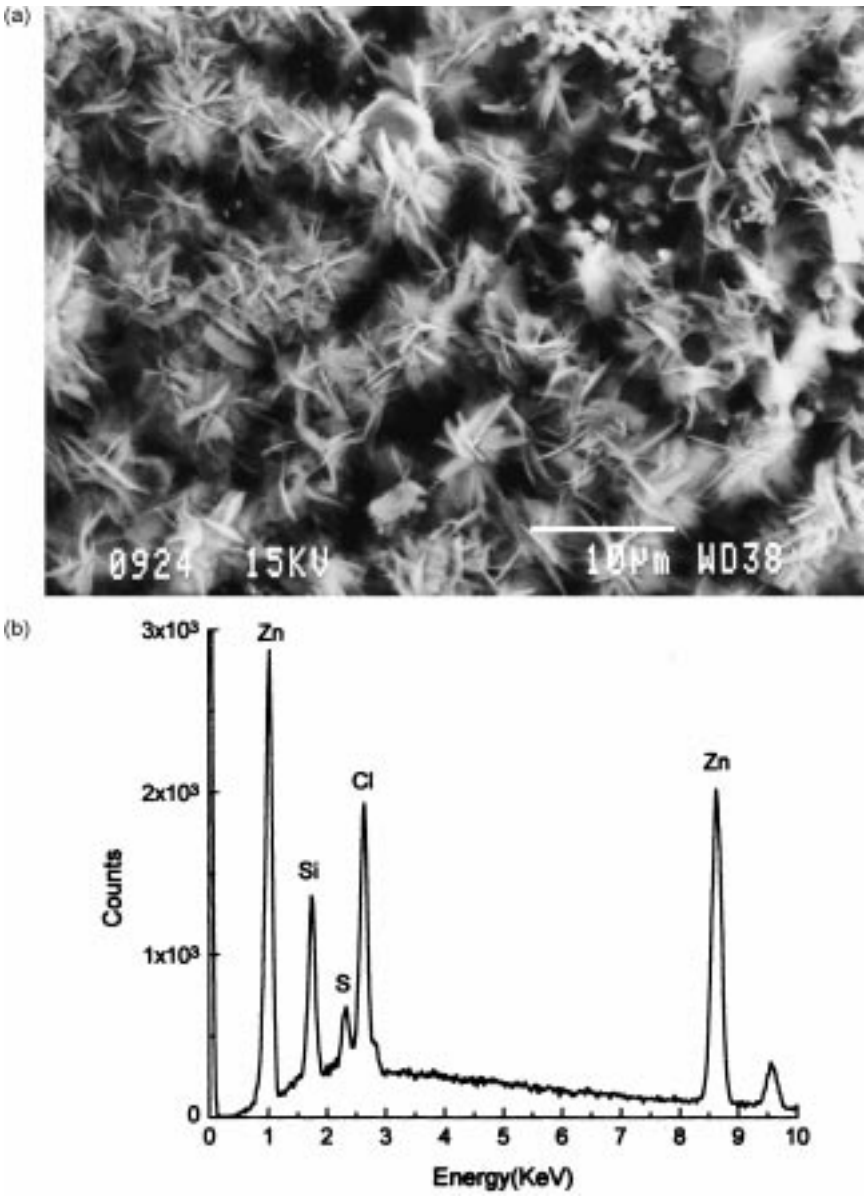

Fig. 3. (a) SEM image: appearance of oxide layer formed in the galvanised steel after 30 days in NaCl and (b) EDS spectrum shows that the main compounds of this layer are Zn and Cl.

In Fig. 6, the linear polarisation curves corresponding to the samples of the two materials in aerated 3.5% NaCl solution with different amounts of $CeCl_3$ are presented. As can be observed in all cases, the effect of the presence of the lanthanide salt in the electrolyte causes a displacement of the cathodic branch toward lower

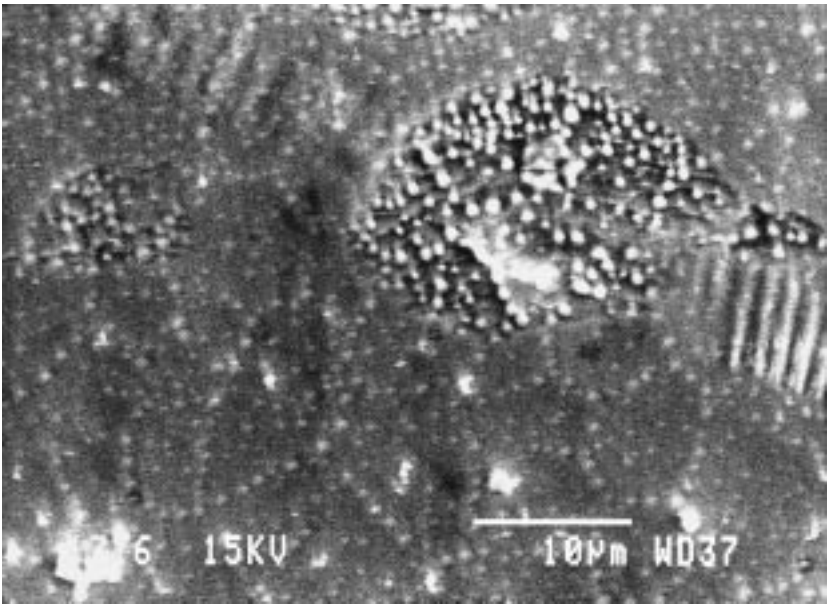

Fig. 4. SEM micrograph: attacked appearance of galvanised steel after carrying out a linear polarisation curve in NaCl solution.

current densities as well as a decrease in the corrosion potential of the system. Both events bring about a reduction in the activity of the system, characteristic of the behaviour of cathodic inhibitors [22–25].

In order to identify the inhibition mechanism that occurs in the aluminium alloy, its surface appearance was observed after 2 h of immersion in a solution of 3.5% NaCl with 500 ppm of $CeCl_3$ (Fig. 7(a) and (b)). In this figure, the presence of some nodular areas can be observed that are clearly distinguishable from the rest of the surface, and whose EDS spectrum (Fig. 7(c)) shows that an accumulation of cerium exists in these nodules. When analysing the substrate under the cracks present in the nodular areas (Fig. 7(d)), we can appreciate how the cerium-rich precipitates have been deposited on intermetallic compounds of Al_6–(Mn,Fe,Cr). As commented previously, these intermetallic compounds display cathodic character with respect to the matrix. To this effect, a high concentration of OH^- ions is generated on them in the first stage of the corrosion process. These ions react with the cations Ce^{3+} giving rise to an insoluble oxide/hydroxide that precipitates on the intermetallic compounds, inhibiting the cathodic reaction. A mechanism of this type for aluminium–copper alloys has been described by other authors [26]. In this way, when the cathodic areas are blocked, it is possible to eliminate the process of local corrosion, even for samples exposed for 30 days (Fig. 8).

In the case of galvanised steel, a fine yellow coating with microcracks (Fig. 9) is observed on the samples after immersion in the inhibitor solution. These microcracks were possibly formed in the drying process of the sample. The formation of a

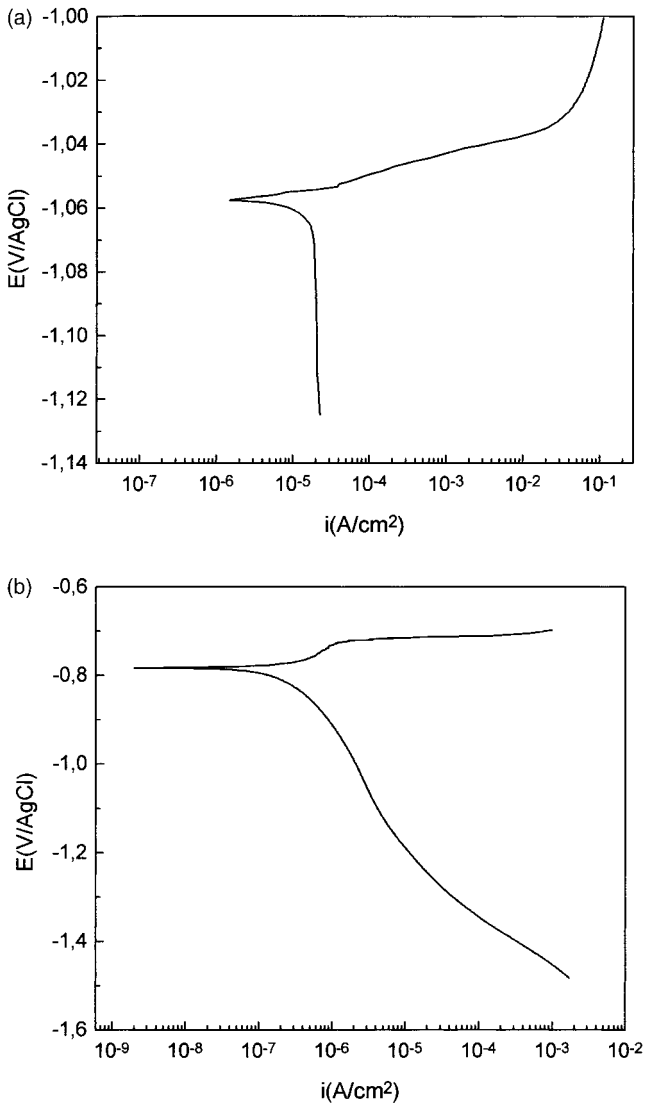

Fig. 5. Linear polarisation curves for (a) galvanised steel, and (b) AA5083 alloy, at a sweep rate of 0.16 mV s^{-1} in NaCl solution.

conversion coating of this type over the whole surface of the sample is due to the process of uniform corrosion of the galvanised steel in which the anodic and cathodic areas are exchanged continuously. Zn, Cl and Ce have been detected in this film by EDS (Fig. 10).

The production of OH^- anions in the cathodic reaction produces areas with a local alkaline pH that favours the cerium precipitation. This reaction competes with

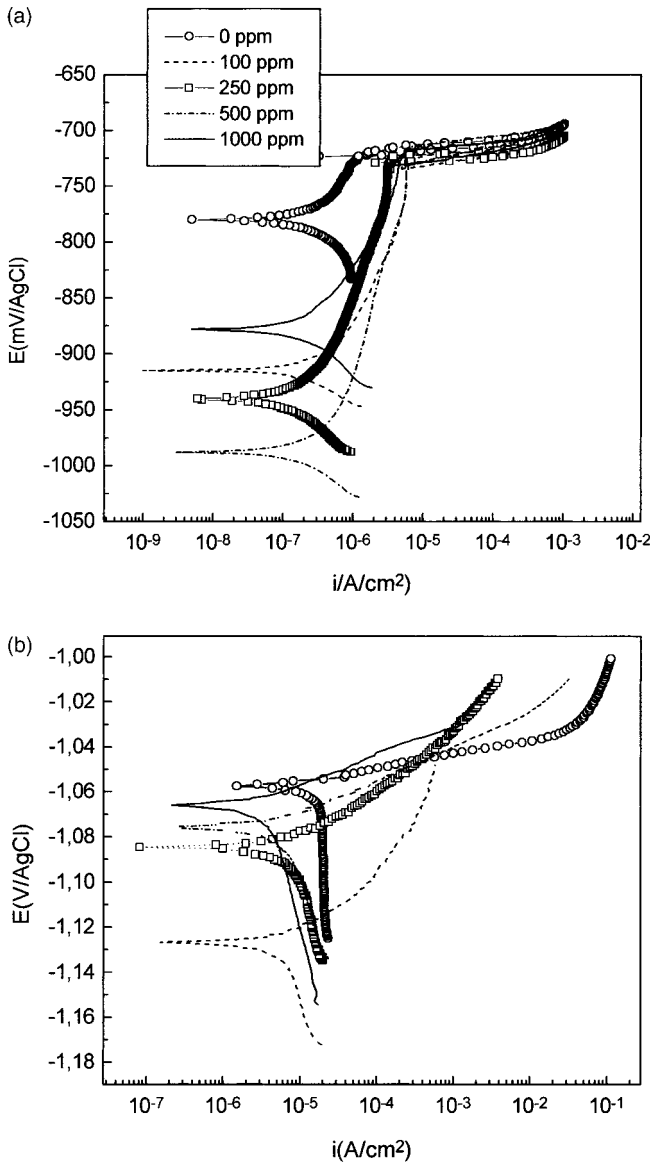

Fig. 6. Linear polarisation plots in 3.56% NaCl solution with different amounts of $CeCl_3$ for (a) aluminium alloy and (b) galvanised steel.

the formation of zinc hydroxide, explaining the large quantity of zinc detected in the film formed.

The film colouration could be due to the presence of cerium as Ce^{4+}, as a consequence of the oxidation of the Ce^{3+}. In a previous work [27], the authors observed

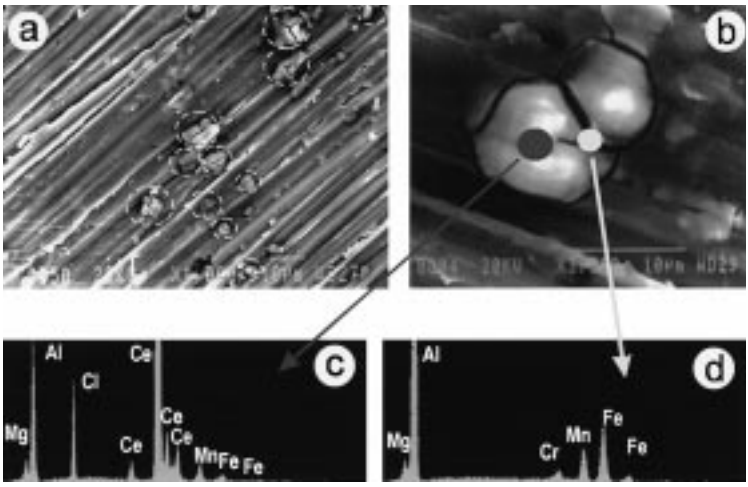

Fig. 7. (a) SEM micrograph recorded on a sample of AA5083 alloy after 2 h of immersion in a solution of 3.56% NaCl with 500 ppm of $CeCl_3$, (b) high magnification view of one of the nodules observed in (a), (c) EDS spectrum of the nodules and (d) components of the substrate under the cracks (marked in (b)).

by means of XPS that the cerium-rich film was formed by a mixture of oxides/hydroxides of Ce(III) and Ce(IV), (CeO_2, $Ce(OH)_4$, and $Ce(OH)_3$). The oxidation state of the cerium is extremely sensitive to the quantity of dissolved oxygen and the pH of the solution. This confirms the coexistence of both oxidation states of the cerium in the film. According to Hinton et al. [21], the presence of H_2O_2 is necessary for the oxidation of Ce^{3+} to Ce^{4+}, and it will be formed as an intermediate species during the process of oxygen reduction. In fact, the existence of H_2O_2 during the corrosion of zinc in an aqueous solution saturated with oxygen is proved in Ref. [23].

Besides this, the phenomenon of "overprecipitation" of cerium particles in some areas of the surface is observed (Fig. 11). This could be due to a loss in the film coherence when it reaches a critical thickness. According to Geary and Bresling [28], the overprecipitation can be explained by the existence of submicrocracks in the conversion film covering the surface that allow the continuation of the anodic and cathodic processes.

The yellow colouration has not been detected, at least not at first inspection, on the surface of AA5083 alloy samples. On one hand, the possible presence of Ce^{4+} compounds should be located on the cathodic precipitates. This colouration would be undetectable for these precipitates because of their microscopic size. Nevertheless, the hypothesis that oxidation state change is indicated in Refs. [14,26] for an Al–Cu alloy with a very similar behaviour to the alloy used in the present work.

4. Conclusions

The corrosive behaviour of the AA5083 alloy and galvanised steel samples in 3.5% NaCl solution has been studied. According to the results obtained, in the alu-

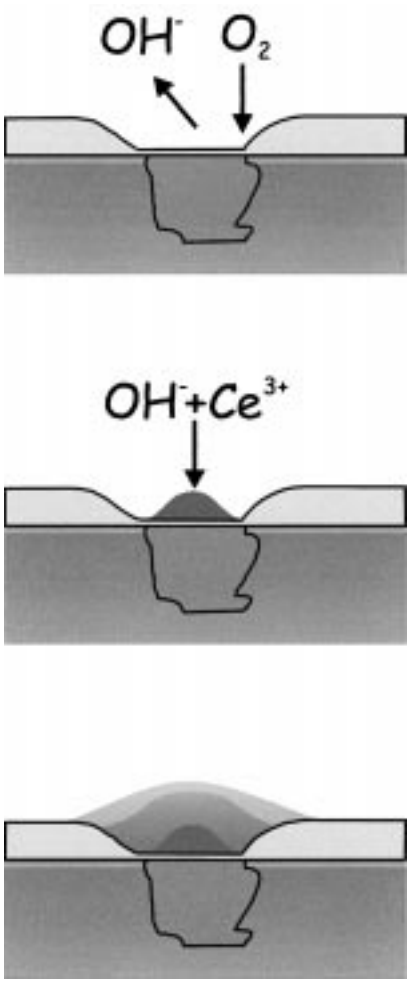

Fig. 8. The corrosion process scheme that the aluminium alloy undergoes.

minium–magnesium alloy, a process of local corrosion prevails in the areas immediately surrounding the intermetallic compound of Al_6–(Mn,Fe,Cr). These compounds are cathodic with respect to the metallic matrix and as such they act as sites for the reduction reaction of O_2. This causes a local increase of the pH, first resulting in the dissolution of the oxide layer surrounding the precipitates, and then the matrix immediately around them.

Regarding the galvanised steel, the presence of lead particles has been detected on its surface by microstructure study. The characterisation of attacked samples shows that these particles do not act as permanent cathodes. Hence, the material corrodes uniformly.

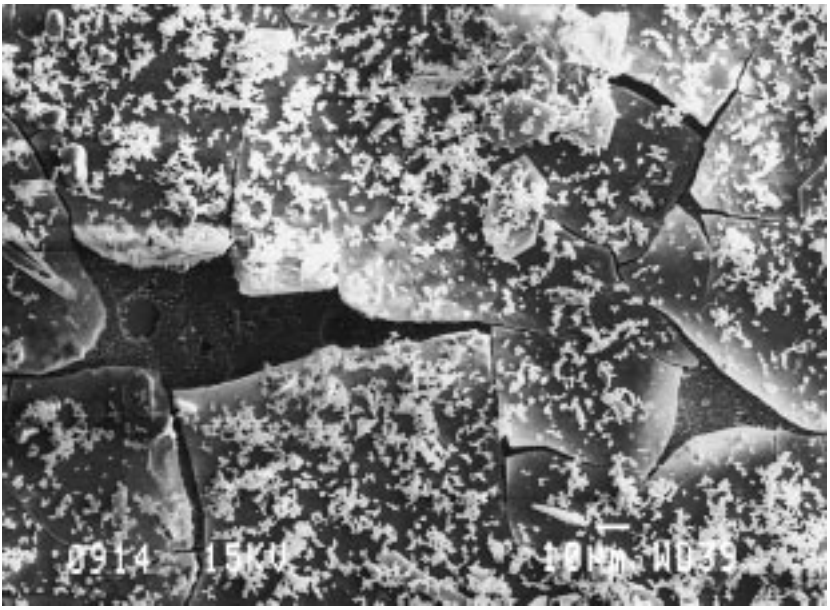

Fig. 9. Surface appearance of galvanised steel after 30 days of immersion in 3.56% NaCl solution with 500 ppm $CeCl_3$.

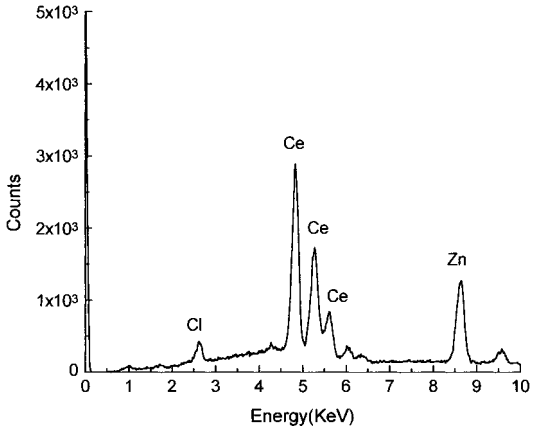

Fig. 10. EDS spectrum of the film formed on galvanised steel samples after 30 days of immersion in the inhibitor solution.

The characteristics of the predominant process of corrosion in each case determine the inhibition mechanism followed when $CeCl_3$ is added to the corrosive environment. In this way, the corrosion of the AA5083 alloy is inhibited by the precipitation of cerium compounds on the Al_6–(Mn,Fe,Cr) intermetallics that act as

Fig. 11. SEM image of large cerium precipitates created in the galvanised steel surface after 30 days in 3.56% NaCl solution with 250 ppm $CeCl_3$ (×500).

permanent cathodes. For the galvanised steel, the formation of a continuous cerium-rich film has been observed. This is due to the exchange of the electrochemical nature of the anodic and cathodic areas with time. As a result of the presence of Ce^{4+} in the film, these samples acquire a characteristic colouration. This film is formed by cerium oxides/hydroxides.

Acknowledgements

The authors wish to thank the CICYT for funding the research project MAT 97-1075-003-02.

References

[1] J. Holmes, Metal Finishing 87 (11) (1989) 65.
[2] Toxicological Profile for Chromium, Agency for Toxic Substances, US Public Health Service, Report no. ATSDR/TP-88/10, 1989.
[3] M. Bethencourt, F.J. Botana, J.J. Calvino, M. Marcos, M.A. Rodríguez-Chacón, Corros. Sci. 40 (11) (1998) 1803.
[4] S. Virtanen, M.B. Ives, G.I. Sproule, P. Schmuki, M.J. Graham, Corros. Sci. 39 (10–11) (1997) 1897.
[5] D.R. Arnott, B.R. Hinton, N.E. Ryan, Corrosion 45 (1989) 12.
[6] F. Mansfeld, Y. Wang, Br. Corros. J. 29 (3) (1994) 194.

[7] A. Aballe, M. Bethancourt, F. Botana, M. Marcos, J. Pérez, M.A. Rodriguez, Rev. Metal. Madrid 33 (6) (1997) 363.
[8] Y.C. Lu, M.B. Ives, Corros. Sci. 37 (1) (1994) 145.
[9] F. Serrano, J.J. de Damborenea, Rev. Metal. Madrid 34 (1998) 127.
[10] L.F. Mondolfo, Aluminium Alloys: Structure and Properties, Butterworths, London, 1976.
[11] M. Bethencourt, F.J. Botana, J.J. Calvino, M. Marcos, J. Pérez, M.A. Rodriguez, The influence of the surface distribution of Al_6(MnFe) intermetallic on the electrochemical response of AA5083 aluminum alloy in NaCl solutions, Mater. Sci. Forum 298–292 (1998) 567–574.
[12] Z. Szklarska-Smialowska, Corros. Sci. 41 (9) (1999) 1743.
[13] G.A. Gehring, M.H. Peterson, Corrosion 37 (4) (1981) 232.
[14] A.J. Aldykiewiccz, H.S. Isaac, A.J. Davenport, J. Electrochem. Soc. 143 (1) (1996) 147.
[15] J.R. Galvele, S.M. de Michelli, I.L. Muller, S.B. de Wexler, I.L. Alanis, Critical potentials for localized corrosion of aluminium alloys, NACE-3, in: R. Staehle, B. Brown, J. Kruger, A. Agrawal (Eds.), National Association of Corrosion Engineers, Houston, USA, 1974, p. 580.
[16] H.E. Biber, Metall. Trans. A 19 (A) (1988) 1603.
[17] F.A. Fasoniyu, F. Weinberg, Metall. Trans. B 21 (B) (1990) 549.
[18] F.C. Porter, Zinc Handbook, Properties, processing and use in desin, in: L.L Faulkner (Ed.), Marcel Dekker, New York, 1991, p. 204.
[19] F.C. Porter, Zinc Handbook, Properties, processing and use in desin, in: L.L Faulkner (Ed.), Marcel Dekker, New York, 1991, p. 214.
[20] F.C. Porter, Corrosion Resistance of Zinc and Zinc Alloys, in: A. Philip, P.E. Shwietzer (Eds.), Marcel Dekker, New York, 1994, p. 61.
[21] B.R.W. Hinton, L. Wilson, Corros. Sci. 29 (8) (1989) 967.
[22] H. Leindheiser Jr., Corrosion, Metals Handbook. Ninth Edition, ASM Ohio, vol. 13, 1987, p. 377.
[23] R.H. Hausler, Corrosion Inhibition and Inhibitors, in: G.R. Brubaker, P.B.P. Phipps (Eds.), Corrosion Chemistry, American Chemical Society, Washington, USA, 1979, p. 263.
[24] D. Harrop, Chemical Inhibitors for Corrosion Control, in: B.G. Clubley (Ed.), Chemical Inhibitors for Corrosion Control, Royal Society of Chemistry, Manchester, UK, 1990, p. 2.
[25] P.C. Thorne, E.R. Roberts, Inorganic Chemistry, Oliver and Boyd, Londres, UK, 1954, p. 418.
[26] H.S. Isaacs, A.J. Aldykiewicz, A.J. Davenport, J. Electrochem. Soc. 142 (10) (1995) 3342.
[27] F. Serrano, J. de Damborenea, Inhibition efficiency of cerium salts on hot dip galvanised steel in saline medium, Proceedings of the European Corrosion Congress, event no. 221, Netherlands, 1998.
[28] M. Geary, C.B. Breslin, Corros. Sci. 39 (8) (1997) 1341.